Silver/polystyrene-coated hollow glass waveguides for the transmission of terahertz radiation

Bradley Bowden,[1] James A. Harrington,[1,*] and Oleg Mitrofanov[2]

[1]*Department of Material Science & Engineering, Rutgers University, 607 Taylor Road, Piscataway, New Jersey 08854, USA*

[2]*Bell Laboratories, Lucent Technologies, 600 Mountain Avenue, Murray Hill, New Jersey 07974, USA*

[*]*Corresponding author: jaharrin@rutgers.edu*

Received August 1, 2007; accepted August 10, 2007;
posted September 6, 2007 (Doc. ID 85769); published October 4, 2007

We have applied techniques developed for IR waveguides to fabricate Ag/polystyrene (PS) -coated hollow glass waveguides (HGWs) for transmission of terahertz radiation. A loss of 0.95 dB/m at 119 μm (2.5 THz) was obtained for a 2 mm bore, 90 cm long Ag/PS HGW. We found that TE modes are supported in HGWs with thin PS films, while hybrid (HE) modes dominate when PS film thickness increases. The lowest losses are obtained for the thicker PS films and the propagation of the HE modes. © 2007 Optical Society of America

OCIS codes: 060.2280, 060.2310, 140.3070.

There is an increasing use of terahertz (THz) radiation in a variety of applications, including imaging, remote sensing and security screening, and spectroscopy [1]. The functionality of systems that employ THz radiation might be improved if a low-loss, flexible waveguide were available. For example, a low-loss waveguide with good mode selectivity can be used as a cavity for gas sensors and nonlinear applications. Many approaches have been taken to fabricate a THz waveguide, including solid-core polymer fibers [2], photonic crystal fibers [3,4], hollow polymer fibers [5], Bragg fibers [6,7], metal tubes [8], sapphire fibers [9], and metal wires [10]. Our earlier work involved the deposition of Ag or Cu coatings inside polycarbonate tubing to form THz waveguides [11]. Specifically, we measured a loss of 3.9 dB/m at 158.5 μm (1.89 THz) for a 3 mm bore Cu-coated hollow polycarbonate waveguide. To reduce the loss, it is necessary to deposit a dielectric coating over the metallic film as has been done in the IR region, where, for example, an AgI film was deposited over an Ag metal film [12]. We have chosen to deposit polystyrene (PS) films over Ag films, as PS has a low loss at THz frequencies.

A significant challenge in extending metal/dielectric, hollow waveguide technology to THz frequencies is that a much thicker dielectric layer is required for low loss. This may be seen from Eq. (1), which shows that for the HE_{11} mode the optimum dielectric layer thickness, d_d, is proportional to the design wavelength, λ_o:

$$d_d = \frac{\lambda_o}{2\pi\sqrt{{n_d}^2 - 1}} \tan^{-1}\left[\frac{n_d}{({n_d}^2 - 1)^{1/4}}\right], \qquad (1)$$

where n_d is the refractive index of the dielectric [12]. The wavelength of THz radiation is 10 to 100 times longer than IR radiation; hence a corresponding increase in film thickness is necessary to achieve low loss.

To prepare THz hollow glass waveguides (HGWs), an Ag film is first deposited within a glass substrate tube by combining a solution containing $AgNO_3$ and NH_4OH with a reducing solution containing dextrose and Na_2EDTA. The glass tubes had bore dimensions of 1.6, 1.7, and 2.2 mm and were 120 cm long. The Ag film grows at a rate of approximately 1 μm/h, and our Ag films were normally about 1 μm thick. This is much thicker than the skin depth for Ag at THz frequencies (100 nm at 119 μm); therefore, no THz radiation will penetrate the HGW wall. The PS films were deposited over the Ag coatings by using a liquid-flow coating process [13] in which a PS/toluene solution is drawn through the HGW at a constant coating velocity by a peristaltic pump. Typical parameters that we used were a coating velocity of 4 cm/min, a concentration of 25 wt. % PS, and a viscosity of 0.23 Pa s.

The spectrum of a Ag/PS HGW exhibits interference peaks at wavelengths, λ_m, given by

$$\lambda_m = \frac{d_{ps}(4\sqrt{n^2 - 1})}{m}, \qquad (2)$$

where d_{ps} is the thickness of the PS film, n is the refractive index of the PS film, and m is a positive integer that corresponds to the order of the interference peak [13]. Rearranging Eq. (2), we obtain an expression for d_{ps} in terms of the difference in wavenumber, $\tilde{\nu}_m - \tilde{\nu}_{m-1}$, between any two adjacent interference peaks,

$$d_{ps} = \frac{(\tilde{\nu}_m - \tilde{\nu}_{m-1})^{-1}}{4\sqrt{n^2 - 1}}. \qquad (3)$$

We do not have a broadband THz spectrometer, so we use the spectral response of the Ag/PS HGW in the near IR to calculate the PS film thickness.

Figure 1 shows the absorption as a function of

0146-9592/07/202945-3/$15.00

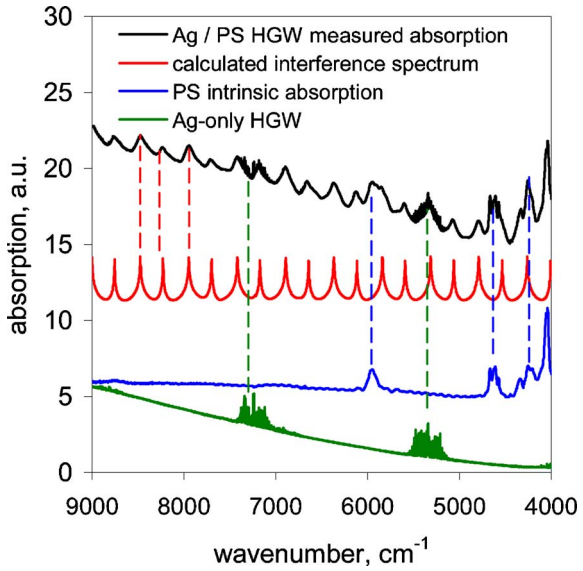

Fig. 1. (Color online) Near-IR absorption spectrum of a 1.7 mm bore diameter Ag/PS HGW (top trace, black) is compared with the absorption spectra of an Ag-only HGW (bottom trace, green), a free-standing PS film (second from bottom, blue), and the calculated interference spectrum for a 7.7 μm thick PS layer on Ag (second from top, red). The vertical scale is offset for clarity.

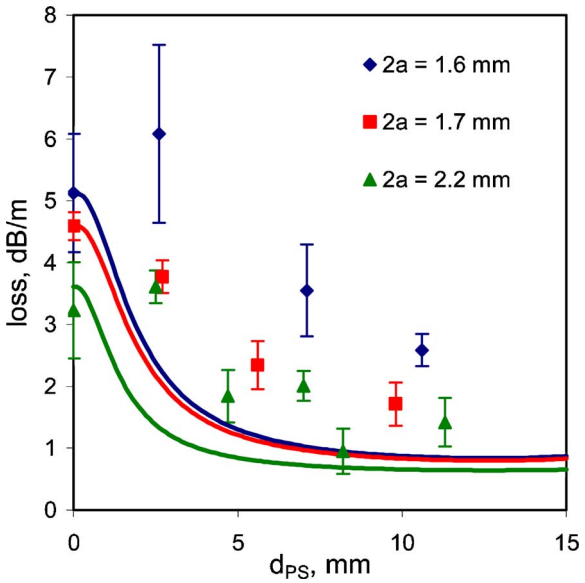

Fig. 2. (Color online) Measured transmission loss plotted as a function of PS film thickness, d_{ps}, for 119 μm radiation propagating in 1.6 mm (top curve, blue), 1.7 mm (center curve, red), and 2.2 mm (bottom curve, green) bore diameter Ag/PS-coated HGWs.

wavenumber for an Ag/PS-coated HGW fabricated by using a 22.5% PS/toluene solution and a coating rate of 6.1 cm/min. There are nine interference peaks between 8770 and 6380 cm^{-1}, so the average spacing between adjacent peaks is 266 cm^{-1}. Assuming that the refractive index of PS is 1.58 and substituting 266 cm^{-1} for $\tilde{\nu}_m - \tilde{\nu}_{m-1}$ in Eq. (3), the calculated PS film thickness is 7.7 μm. The calculated interference spectrum for a 7.7 μm PS film on Ag is also shown in Fig. 1 along with the absorption spectra of a free-standing PS thin film and an Ag-only HGW. Dashed lines connect some of the features that each spectrum has in common with that of the Ag/PS HGW. Atmospheric absorption peaks occur at 5400 and 7300 cm^{-1}, and the increase in absorption with increasing wavenumber is due to scattering from surface roughness, which varies as λ^{-2}. PS has absorption peaks at 5980, 4670, and 4060 cm^{-1}. From the data in Fig. 1 we see that the calculated interference spectrum for a 7.7 μm thick PS film on Ag agrees well with the interference peaks observed in the Ag/PS HGW spectrum.

The loss measurements at 119 μm (2.5 THz) were made by using a DEOS SIFIR-50 THz laser. This laser operates by pumping CH_3OH molecules with a CO_2 laser at 9.62 μm, and the output is 25 mW at 119 μm. A cutback technique was used to accurately determine the absorption coefficient for each HGW. In Fig. 2 we show the measured straight loss for different bore sizes as a function of the PS film thickness. Solid curves indicate the theoretical loss of the HE_{11} mode calculated by using the ray optics method. The ray optics calculation is initiated by evaluating the reflectance, R, of the Ag/PS stack at an angle that is equal to the HE_{11} mode angle, θ_z. The loss, α, is given by

$$\alpha = \frac{1-R}{2a\tan(\theta_z)}, \tag{4}$$

where θ_z is measured from the normal to the surface [14]. The complex refractive indices of Ag and PS at 119 μm are $305-i529$ [15] and $1.58-i3.58\times10^{-3}$ [16], respectively. The theoretical calculations assume that the core is a vacuum; 0.5 dB/m is added to the theoretical loss to account for atmospheric absorption at 119 μm [11]. The loss for the Ag/PS HGWs is generally higher than the theoretical HE_{11} mode loss, but the predicted trend of decreased loss with increasing film thickness is demonstrated. The lowest measured loss in air is 0.95 dB/m for a 2.2 mm bore diameter Ag/PS-coated HGW with an 8.2 μm PS film. To our knowledge this is the lowest loss measured to date for a HGW at this wavelength.

The output mode profile for 119 μm radiation propagating in Ag/PS HGWs was studied by using a Spiricon pyroelectric camera. Images were recorded for both horizontal and vertical polarizations by using wire grid polarizers inserted between the output end of the waveguide and the camera. Figure 3 shows the mode profiles of radiation exiting a 1.6 mm bore Ag-only HGW and a Ag/PS HGW with a 10 μm PS film, both 90 cm long. The doughnut shape of the mode profile for the waveguide with no PS film is characteristic of the TE_{01} mode. The horizontally and vertically polarized radiation profiles confirm that the electric field is parallel to the walls of the waveguide, also a characteristic of the TE_{01} mode. In contrast, the mode profile of the Ag/PS-coated HGW with a 10 μm PS film is Gaussian-like, a characteristic of the HE_{11} mode. The horizontal polarization of the source beam is largely maintained in the HGW. In Fig. 3 we also see the results for the 2.2 mm bore

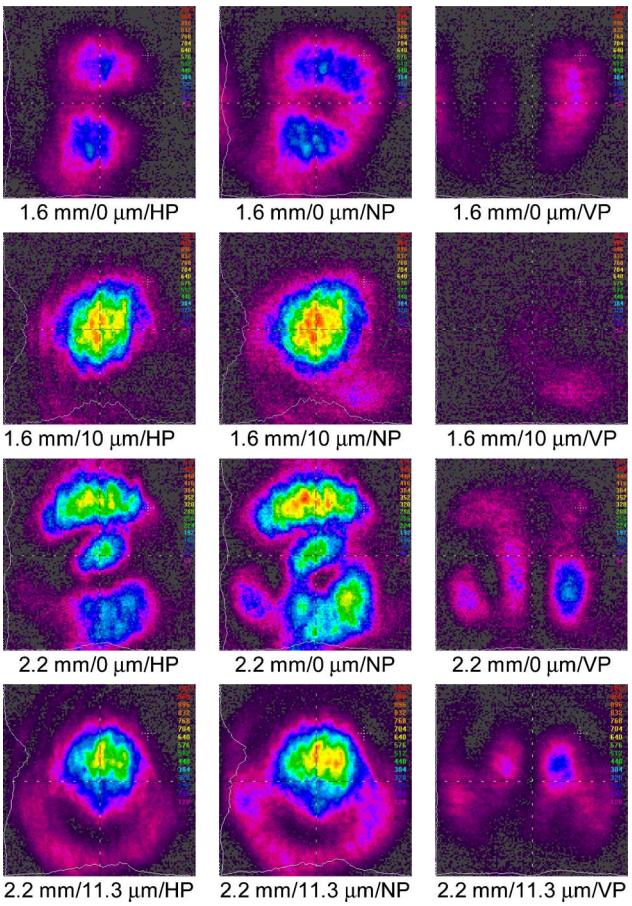

Fig. 3. (Color online) Far-field spatial intensity variation of 119 μm radiation exiting 90 cm long Ag/PS HGWs. The HGW bore diameter, PS film thickness, and polarization state of the collected radiation are indicated below each image. Images are obtained with either a horizontal (HP) or vertical (VP) wire grid polarizer inserted between the waveguide and camera, or no polarizer (NP).

HGWs. Some higher-order modes propagate in the 2.2 mm waveguides that are not present in the 1.6 mm Ag/PS-coated HGWs. The observed increase in the number of propagating modes with increasing waveguide bore diameter is consistent with electromagnetic theory.

At near-glancing incidence metals have high reflectivity for *s*-polarized radiation but low reflectivity for *p*-polarized radiation due to the effect of the metal's principle angle of incidence [17]. The TE_{01} mode propagates with low loss in Ag-coated HGWs with no dielectric coating because the radiation is *s*-polarized with respect to the metal surface. Hybrid modes comprising both *s*- and *p*-polarized radiation are highly attenuated for metal-only HGWs, because the *p*-polarized component is highly attenuated. The addition of the dielectric PS film increases the reflectivity of the metal for *p* polarization via an inference effect, and thus the loss of the hybrid modes decreases. Ray optics calculations predict a minimum HE_{11} mode loss with a 12.7 μm PS film. The transition from TE_{01} dominated transmission to HE_{11} mode transmission as the film thickness increases supports this theory.

For the first time to our knowledge, a low-loss, metal/dielectric HGW has been demonstrated for THz radiation. It was found that Ag/PS-coated HGWs have significantly lower loss for 119 μm radiation as compared with Ag-only HGWs. The dominant transmission mode transitions from TE_{01} for the Ag-only guides to HE_{11} for Ag/PS HGWs with near-optimum PS film thickness. The best waveguide demonstrated in this study is a 2.2 mm bore diameter Ag/PS HGW with an 8.2 μm PS film thickness. The measured transmission loss of this waveguide with an air core is 0.95 dB/m.

References

1. D. Mittleman, *Sensing with Terahertz Radiation* (Springer, 2003).
2. L. J. Chen, H. W. Chen, T. F. Kao, J. Y. Lu, and C. K. Sun, Opt. Lett. **31**, 308 (2006).
3. H. Han, H. Park, M. Cho, and J. Kim, Appl. Phys. Lett. **80**, 2634 (2002).
4. M. Goto, A. Quema, H. Takahashi, S. Ono, and N. Sarukura, Jpn. J. Appl. Phys., Part 1 **43**, 317 (2004).
5. T. Hidaka, H. Minamide, H. Ito, S. Maeta, and T. Akiyama, Proc. SPIE **5135**, 70 (2003).
6. Y. Gao, N. Guo, B. Gauvreau, O. Zabeida, L. Martinu, C. Dubois, and M. Skorobogatiy, J. Mater. Res. **21**, 2246 (2006).
7. M. Skorobogatiy, Opt. Lett. **30**, 2991 (2005).
8. G. Gallot, S. P. Jamison, R. W. McGowan, and D. Grischkowsky, J. Opt. Soc. Am. B **17**, 851 (2000).
9. S. P. Jamison, R. W. McGowan, and D. Grischkowsky, Appl. Phys. Lett. **76**, 1987 (2000).
10. J. Deibel, K. Wang, M. Escarra, and D. Mittleman, Opt. Express **14**, 279 (2006).
11. J. A. Harrington, R. George, P. Pedersen, and E. Mueller, Opt. Express **12**, 5263 (2004).
12. J. A. Harrington, *Infrared Fibers and their Applications* (SPIE, 2003).
13. Y. Abe, Y. Matsuura, Y. W. Shi, H. Uyama, and M. Miyagi, Opt. Lett. **23**, 89 (1998).
14. M. Miyagi, J. Lightwave Technol. **LT-3**, 303 (1985).
15. M. A. Ordal, L. L. Long, R. J. Bell, S. E. Bell, R. R. Bell, R. W. Alexander, Jr., and C. A. Ward, Appl. Opt. **22**, 1099 (1983).
16. J. R. Birch, Infrared Phys. **33**, 33 (1992).
17. E. Hecht, *Optics* (Addison Wesley, 2002).